METABOLISM



# An engineered *E. coli* Nissle improves hyperammonemia and survival in mice and shows dose-dependent exposure in healthy humans

**Caroline B. Kurtz[1]*, Yves A. Millet[1†], Marja K. Puurunen[1], Mylène Perreault[1], Mark R. Charbonneau[1], Vincent M. Isabella[1], Jonathan W. Kotula[1‡], Eugene Antipov[1], Yossi Dagon[1], William S. Denney[2], David A. Wagner[3], Kip A. West[1], Andrew J. Degar[4], Aoife M. Brennan[1], Paul F. Miller[1]**

**The intestine is a major source of systemic ammonia ($NH_3$); thus, capturing part of gut $NH_3$ may mitigate disease symptoms in conditions of hyperammonemia such as urea cycle disorders and hepatic encephalopathy. As an approach to the lowering of blood ammonia arising from the intestine, we engineered the orally delivered probiotic *Escherichia coli* Nissle 1917 to create strain SYNB1020 that converts $NH_3$ to L-arginine (L-arg). We up-regulated arginine biosynthesis in SYNB1020 by deleting a negative regulator of L-arg biosynthesis and inserting a feedback-resistant L-arg biosynthetic enzyme. SYNB1020 produced L-arg and consumed $NH_3$ in an in vitro system. SYNB1020 reduced systemic hyperammonemia, improved survival in ornithine transcarbamylase–deficient *spf*$^{ash}$ mice, and decreased hyperammonemia in the thioacetamide-induced liver injury mouse model. A phase 1 clinical study was conducted including 52 male and female healthy adult volunteers. SYNB1020 was well tolerated at daily doses of up to $1.5 \times 10^{12}$ colony-forming units administered for up to 14 days. A statistically significant dose-dependent increase in urinary nitrate, plasma $^{15}$N-nitrate (highest dose versus placebo, $P = 0.0015$), and urinary $^{15}$N-nitrate was demonstrated, indicating in vivo SYNB1020 activity. SYNB1020 concentrations reached steady state by the second day of dosing, and excreted cells were alive and metabolically active as evidenced by fecal arginine production in response to added ammonium chloride. SYNB1020 was no longer detectable in feces 2 weeks after the last dose. These results support further clinical development of SYNB1020 for hyperammonemia disorders including urea cycle disorders and hepatic encephalopathy.**

## INTRODUCTION

The field of synthetic biology has expanded greatly over the past decade, enabling the development of new therapeutic strategies using engineered microbes for the treatment of various diseases, including immunological and metabolic disorders, cancer, infectious diseases, and inborn errors of metabolism (*1*). Microbes have been engineered to produce cytokines, to inhibit pathogenic bacteria, and to secrete therapeutic agents designed for site-specific delivery, yielding promising preclinical results in animal disease models (*1*–*7*).

The mammalian intestinal tract is inhabited by a dense community of microorganisms and is a possible target for the development of a new class of live microbial therapeutics designed to modulate toxic dietary or endogenous gut-derived metabolites (*8*, *9*). Engineered probiotics may be uniquely suited to consume toxic metabolites in the intestine and convert them to nontoxic forms. Multistep metabolic pathways can be engineered into bacteria to enhance the consumption and breakdown of metabolites in the location they are formed. Ammonia ($NH_3$) is a toxic metabolite that is generated in both the small intestine and the colon and enters the portosystemic circulation (*10*–*12*). Elevated circulating ammonia not metabolized to urea by the liver can cross into the brain and induce astrocyte swelling, edema, and neurotoxicity through increased reactive oxygen species and inflammatory responses (*13*). Similar quantities of ammonia are generated in the small and large intestine (*10*), but the mechanisms of ammonia generation differ. Small intestinal ammonia arises from the deamidation of glutamine within intestinal epithelial cells (*14*, *15*), whereas bacterial degradation of protein and microbial urease activity generates ammonia in the colon (*16*, *17*).

The metabolism of ammonia and subsequent renal elimination is predominantly reliant on a functional liver. Ammonia entering the liver from the portal circulation is metabolized by urea cycle enzymes expressed primarily in periportal hepatocytes (*18*). Hyperammonemia occurs when there is a defect in ammonia-detoxifying enzymes, such as in urea cycle disorders (UCDs), or when the liver is damaged, as in cirrhosis (*19*, *20*). UCDs are rare but serious and potentially fatal genetic diseases characterized by a deficiency in one of the six enzymes or two transporters necessary for the urea cycle to effectively metabolize waste nitrogen to urea (*21*). For patients with UCD, complete or partial defects in the enzymatic pathway result in ineffective metabolism of waste nitrogen and its toxic accumulation in the form of ammonia. Despite pharmacological treatment with ammonia scavengers and dietary management, patients continue to suffer from hyperammonemic crises. Hepatic encephalopathy (HE) comprises a heterogenous group of disorders stemming from liver damage and is characterized by declining neurocognitive function (*22*, *23*). HE occurs in 30 to 40% of patients with cirrhosis (*24*). The prevalence of cirrhosis in the United States was estimated in 2015 to be 0.27% of the population or 633,323 adults (*25*). Many of these patients will be diagnosed after an acute episode requiring hospitalization, and the 1-year mortality rate for such patients is

[1]Synlogic Inc., 301 Binney Street, Cambridge, MA 02142, USA. [2]Human Predictions LLC, 649 Massachusetts Avenue Suite 6, Cambridge, MA 02139, USA. [3]Metabolic Solutions Inc., 460 Amherst Street, Nashua, NH 03063, USA. [4]Diversigen Inc., 1 Baylor Plaza, Houston, TX 77030, USA.
*Corresponding author. Email: caroline@synlogictx.com
†Present address: Kaleido Biosciences, 65 Hayden Avenue, Lexington, MA 02421, USA.
‡Present address: Caribou Biosciences, 2929 7th Street, Suite 105, Berkeley, CA 94710, USA.

about 50%; thus, the burden of the disease is high. The more severe form of HE, referred to as overt HE, is associated with obvious mental disorientation and physical symptoms (for example, asterixis, lethargy, seizures, tremors, stupor, or coma) that arise over several days or hours and may be fatal (*26*). The pathogenesis of HE is believed to be largely attributable to hyperammonemia and inflammatory processes associated with damage to the liver (*27*, *28*). Increased arterial and venous ammonia concentrations correlated with increased HE severity, with concentrations above 100 μM in addition to model for end-stage liver disease (MELD) scores above 32 that are predictive of an onset of an episode of HE with 94% specificity and 74% accuracy (*29*, *30*).

The long-standing evidence for the importance of intestinally generated ammonia and the observation that antibiotic treatment can lower systemic and portal ammonia (*31*–*33*) have led to the clinical development of therapeutic agents aimed at decreasing gut microbial activity or adsorbing colonic ammonia for the treatment of HE (*22*, *23*). Those drugs include the antibiotic rifaximin, which may reduce activity of urease-producing bacteria, and the laxative lactulose, a nonabsorbable disaccharide that acidifies the colon and decreases transit time, resulting in increased fecal elimination of ammonia (*34*). Patients with HE have poor compliance with available treatment regimens due to the complexity of dosing (for example, lactulose must be self-titrated until three bowel movements per day are produced), and side effects of treatment can lead to poor adherence to therapy (diarrhea, dehydration, hyponatremia, abdominal pain, and headache). Investigational agents that may scavenge intestinal ammonia, such as AST-120, a suspension of activated carbon microspheres acting as an ammonia adsorbent in the gut, have been explored preclinically and in patients with HE (*35*). More recently, a microbiome-based approach that replaces the gut microbiota with a defined consortium of bacteria with low urease activity has been explored in a preclinical model of hyperammonemia and showed prolonged lowering of colonic ammonia production and decreased mortality in mice (*6*). Strains of *Escherichia coli* have previously been modified to convert ammonia to amino acids such as arginine (*36*), but characterization of their ammonia assimilation potential in vivo has thus far not been considered. Therefore, the limitations in current standard of care treatments for hyperammonemia and the lack of new agents highlight the need for development of a safe, well-tolerated, and effective treatment to improve outcomes for conditions such as UCD and HE (*37*, *38*).

Applying principles of drug development, including dose response, pharmacokinetics, and clearance, is particularly challenging in the field of microbial therapies because they consist of living organisms, are confined to the gut, and are potentially capable of replicating or losing viability as they transit the gastrointestinal (GI) tract. Detection of therapeutic organisms in the background of the host microbial flora is also challenging. Sampling from the gut in an intact host is not feasible (except for collecting feces), making detection of microbial viability and activity challenging and indirect relative to the site of action. Leveraging the safety and tolerability of probiotics in human populations and specific tools of synthetic biology, we sought to address these issues by designing a modified probiotic to perform specific metabolic functions needed by the patient. The specific detection of our strain within the microbiome and the application of principles of pharmacodynamics and pharmacokinetics in preclinical and clinical studies were possible based on the engineered features of this strain.

We selected *E. coli* Nissle 1917 (EcN) as the chassis organism because of its long history of safe use in human populations and the availability of numerous tools for genetic manipulation in this species (*39*). EcN is widely used in Europe as a probiotic under the brand name Mutaflor. The excretion profile of orally dosed EcN was recently evaluated in healthy volunteers, where the median clearance time was 1 week, with 80% of healthy volunteers having cleared by 3 weeks (*40*). This is beneficial when considering the use of a probiotic therapeutically, because it is not expected to colonize the host or substantially alter the microbiome. The safety, tolerability, and efficacy of chronic daily EcN treatment has also been evaluated in multiple long-term (up to 12 months), placebo-controlled clinical trials in patients with inflammatory bowel disease and irritable bowel syndrome (*41*–*44*). In these studies, EcN was well tolerated, with adverse effects similar to placebo or comparator (mesalamine); thus, daily treatment with EcN for chronic disorders is feasible.

The objective of this study was to design, characterize, and evaluate the safety and tolerability of an engineered EcN, SYNB1020, for the treatment of disorders of hyperammonemia. SYNB1020 can respond to its environment (anaerobic environment of the GI tract) to consume ammonia and convert it to L-arginine (L-arg), making it well suited for the potential clinical management of hyperammonemia. Arginine is a key intermediate in the urea cycle and is a dietary supplement that is used to treat patients with UCDs (except arginase deficiency). It is often given at high doses (250 mg/kg per day) for treatment of acute decompensation during hyperammonemic crises, with no reported toxicity (*45*, *46*). Enhancement of L-arg biosynthesis was targeted on the basis of the high nitrogen content of L-arg (four atoms of nitrogen) and the positive effect of L-arg supplementation on ureagenesis in several UCDs (*45*, *46*). We confirmed that SYNB1020 efficiently produced arginine from ammonia, lowered ammonia in preclinical models of hyperammonemia, and was well tolerated preclinically and in healthy human volunteers. Translational studies demonstrated the potential of this strain to operate from the GI tract in both preclinical models of hyperammonemia as well as in the clinic. These data serve as proof of concept to support therapeutic strategies based on engineered microbes operating from the intestinal tract to modulate systemic disease.

## RESULTS

### SYNB1020 consumes ammonia and produces arginine

SYNB1020, an engineered EcN strain, was created to convert $NH_3$ to L-arg under anaerobic conditions (see strain schematic in Fig. 1A and list of engineered strains in Table 1) to increase its ability to assimilate ammonia in the oxygen-limited environment of the gut. To maximize arginine production and prevent inhibitory feedback, we deleted the gene encoding the arginine repressor ArgR and then integrated the gene *argA215*, encoding ArgAY19C, a feedback-resistant version of the *N*-acetylglutamate synthase enzyme ArgA ($argA^{fbr}$) (*36*, *47*, *48*), into the intergenic region separating the *malE* and the *malK* genes under the control of the *fnrS* promoter ($P_{fnrS}$), an endogenous anaerobic-inducible promoter found in *E. coli (7)*. Controlling expression of *argA215* anaerobically is an essential aspect of our strain design, and we selected $P_{fnrS}$ for its strong and specific activation under anaerobic conditions similar to those found in the colon (*7*, *49*, *50*). We subsequently confirmed activation of the $P_{fnrS}$ in vivo in the mouse gut (fig. S1).

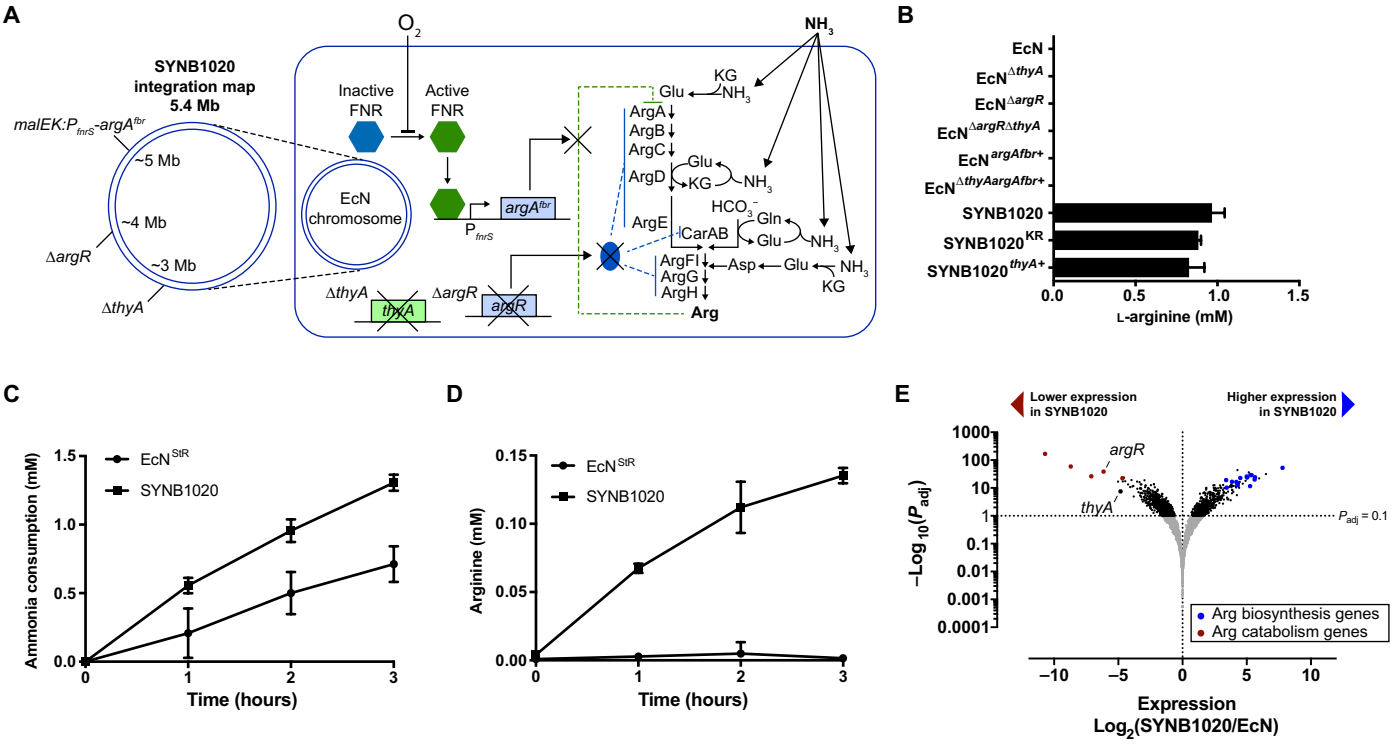


**Fig. 1. Characterization of SYNB1020.** (**A**) Schematic of the engineered strain SYNB1020, including its intended effect on L-arg metabolism. (**B**) L-arg production by engineered strains in vitro. Data represent measurements from three independent bacterial cultures ± SD. *P* values described in the text were generated using two-tailed unpaired Student's *t* test. (**C**) Strain activity was tested in modified M9 medium supplemented with 5 mM ammonia. Assay reactions contained chloramphenicol (10 μg/ml) to inhibit ammonia consumption due to cell division and de novo protein synthesis. SYNB1020 cells were induced by incubation at low oxygen (EcN$^{StR}$ was treated in a similar manner). Ammonia consumption by EcN$^{StR}$ and SYNB1020 was quantified using the indophenol-blue method. (**D**) Arginine production by the same samples in (C) was quantified using liquid chromatography–tandem mass spectrometry after derivatization with dansyl-chloride. Data are representative of triplicate measurements ± SD. (**E**) Volcano plot of gene expression in SYNB1020 as compared to EcN, under microaerobic conditions in the presence of thymidine. Genes with an adjusted *P* value ($P_{adj}$) of less than 0.1, as reported by DESeq2, were considered differentially expressed. ArgB, acetyl glutamate kinase; ArgC, *N*-acetyl glutamylphosphate reductase; ArgD, *N*-acetylornithine aminotransferase; ArgE, acetylornithine deacetylase; ArgFI, ornithine carbamoyltransferase; ArgG, arginosuccinate synthase; ArgH, arginosuccinate lyase; CarAB, carbamoyl phosphate synthetase; fbr, feedback resistant; FNR, "fumarate and nitrate reduction" transcription regulator; Gln, glutamine; Glu, glutamate; $HCO_3^-$, bicarbonate; KG, ketoglutarate; *malEK*, intergenic region between *malE* and *malK* genes; Δ*thyA*, thymidylate synthase deletion.

We further modified the resulting arginine-producing strain by deleting the essential thymidylate synthase gene *thyA* that restricts replication within and outside the host when thymidine concentrations are low (*51*). As expected, the newly generated strain SYNB1020 had impaired growth in the absence of thymidine supplementation (Table 1and fig. S2). Both the *argR* deletion and the expression of *argA*$^{fbr}$ were necessary for L-arg production, as demonstrated by the absence of L-arg production in strains lacking either component alone (Fig. 1B). The clinical development strain, SYNB1020, lacks any antibiotic resistance genes in compliance with U.S. Food and Drug Administration regulations on live therapeutics (*52*). We inserted a gene conferring kanamycin resistance into the genome of SYNB1020 to create a proxy strain, SYNB1020$^{KR}$, that could be used in preclinical studies for isolation from complex microbial samples such as fecal homogenate. SYNB1020$^{KR}$ could be selected on agar containing kanamycin but was otherwise identical to SYNB1020. In vitro testing showed that deleting *thyA* had no impact on L-arg production ($P = 0.12$ and $P = 0.37$ comparing SYNB1020 to SYNB1020$^{thyA+}$ or SYNB1020$^{KR}$, respectively; Table 1 and Fig. 1B). The increased in vitro ammonia consumption by SYNB1020 compared to the unengineered streptomycin-resistant strain EcN$^{StrR}$ could be explained almost entirely by L-arg production (Fig. 1, C and D). Over 3 hours, SYNB1020 consumed 0.59 μmol more of ammonia than EcN$^{StrR}$ (Fig. 1C). In that time, SYNB1020 produced 0.13 μmol of L-arg (Fig. 1D), which corresponds to consumption of 0.52 μmol of ammonia (1 mol of L-arg contains 4 mol of ammonia).

## SYNB1020 exhibits increased expression of the arginine biosynthesis pathway and stress response genes

To determine the impact of the genetic modifications implemented in SYNB1020 on gene expression, we performed RNA sequencing on triplicate cultures of EcN$^{StrR}$, SYNB1020, and EcN$^{\Delta thyA}$ after 2 hours of microaerobic induction with thymidine supplementation. Differential gene expression was then determined with DESeq2 (*53*), using correction for multiple hypothesis testing ($\alpha = 0.1$; table S1). The deletions of *argR* and *thyA* in SYNB1020 and *thyA* in EcN$^{\Delta thyA}$ were confirmed in their respective strains by decreased expression of these genes as compared to EcN$^{StrR}$ (Fig. 1E and table S1). In SYNB1020, we observed that every gene in the L-arg biosynthesis pathway exhibited increased expression (Fig. 1E and fig. S3). We also noted decreased expression of an operon encoding an arginine degradation pathway (*arcABCD*) in SYNB1020 as compared to EcN$^{StrR}$ (table S1). Down-regulation of *arcABCD* is consistent with its positive regulation by ArgR, as observed in other bacterial species (*54*, *55*).

**Table 1. Bacterial strains.** EcN was genetically engineered with the described series of changes to create SYNB1020 and related tool strains that we used to elucidate activity in in vitro and in vivo studies.

| Strain | Genotype |
|---|---|
| EcN | *E. coli* Nissle 1917 |
| $EcN^{StrR}$ | EcN, streptomycin resistant |
| $EcN^{KR}$ | EcN, kanamycin resistant |
| $EcN^{\Delta argR}$ | EcN, Δ*argR* |
| $EcN^{\Delta thyA}$ | EcN, Δ*thyA*::$Cm^R$ |
| $EcN^{argAfbr+}$ | EcN, *malEK*::$Cm^R$-$P_{fnrS}$-$argA^{fbr}$ |
| $EcN^{\Delta thyA\ argAfbr+}$ | EcN, Δ*thyA*, *malEK*::$Cm^R$-$P_{fnrS}$-$argA^{fbr}$ |
| $EcN^{\Delta argR\ \Delta thyA}$ | EcN, Δ*argR*, Δ*thyA*::$Cm^R$ |
| $EcN^{\Delta thyA,\ argAfbr+}$ | EcN, Δ*thyA*, *malEK*::$Cm^R$-$P_{fnrS}$-$argA^{fbr}$ |
| EcN-GFP | EcN containing plasmid with $P_{fnrS}$–GFP (green fluorescent protein) transcription fusion |
| $SYNB1020^{thyA+}$ | EcN, Δ*argR*, *malEK*::$P_{fnrS}$-$argA^{fbr}$ |
| SYNB1020 | EcN, Δ*argR*, Δ*thyA*, *malEK*::$P_{fnrS}$-$argA^{fbr}$ |
| $SYNB1020^{KR}$ | EcN, Δ*argR*, Δ*thyA*, *malEK*::$P_{fnrS}$-$argA^{fbr}Kan^R$ |

To understand the effects of the *thyA* deletion on the transcriptional state of EcN, we next examined genes that were differentially expressed in $EcN^{\Delta thyA}$ compared to $EcN^{StrR}$ (table S1). We found that the expression of a number of genes involved in stress responses was increased in $EcN^{\Delta thyA}$, even when the strains were grown in the presence of exogenous thymidine. These genes included a central regulator of the stress response in *E. coli*, *rpoS* (*56*), heat-shock protein genes [*dnaKJE* and *groELS* (*57*)], and multiple acid resistance genes [the glutamate decarboxylase genes *gadA* and *gadB* (*58*) and the glutaminase gene *glsA* (*55*)]. We also observed increased expression of purine and pyrimidine biosynthesis genes in $EcN^{\Delta thyA}$, possibly due to stress on DNA synthesis. These differences in stress response gene expression were also evident in SYNB1020, which similarly lacks *thyA* (table S1). Overall, our analysis revealed that *thyA* deletion in SYNB1020 resulted in gene expression changes and led to a global stress response but this response did not interfere with the transcriptional activation of the L-arg biosynthetic pathway.

## SYNB1020 lowers blood ammonia and increases survival in mouse models of hyperammonemia

To demonstrate that orally delivered SYNB1020 survived transit through the GI tract, we first evaluated the viability of antibiotic-resistant $SYNB1020^{KR}$ under conditions closer to those encountered in vivo. Ex vivo survival assays in cecolonic matrix (cecum and colonic contents combined) demonstrated that $SYNB1020^{KR}$ was able to survive effectively at all doses and time points tested (table S2). Notably, we observed loss in viable cell recovery at the later time points for the $1 \times 10^{10}$ dose, which was likely due to the exhaustion of nutrients and/or thymidine in the ex vivo cecolonic matrix. Similar to ex vivo studies, we observed a dose- and time-dependent increase in $SYNB1020^{KR}$ cecum, colon, and fecal recovery in mice that were orally administered bacteria (table S3 and fig. S4). The cells recovered from mice administered $SYNB1020^{KR}$ were metabolically active, as measured by the production of arginine in cecum and colon (table S4).

To assess the efficacy of SYNB1020 in vivo, we first measured metabolites of arginine in the plasma and urine of mice and nonhuman primates dosed with SYNB1020 or $SYNB1020^{KR}$ as indicators of strain activity. Arginine metabolism is complex, as arginine can be converted into several metabolites, including citrulline, ornithine, proline, and nitric oxide (*59*). Treatment of different strains of mice [C57BL/6 or ornithine transcarbamylase (OTC) $spf^{ash}$(abnormal skin and hair)] or healthy nonhuman primates with SYNB1020 or $SYNB1020^{KR}$ using multiple dosing regimens (single or multiple doses) resulted in variable and inconsistent production of arginine metabolites including ornithine, citrulline, and nitrate (derived from further metabolism of nitric oxide) across experiments (table S5).

We first tested the ability of SYNB1020 and related strains to lower ammonia in vivo in the OTC $spf^{ash}$ murine model of UCD (OTC $spf^{ash}$) (*60*). In this model, a point mutation in the last nucleotide of the fourth exon of the mitochondrial OTC gene reduces the activity of this liver enzyme to 5 to 10% of wild-type animals, leading to the inability to process ammonia efficiently and the subsequent development of hyperammonemia (*60*). We observed that feeding OTC $spf^{ash}$ mice a high-protein diet for 48 hours increased circulating ammonia to toxic levels compared to animals maintained on a standard chow diet (Fig. 2A). Coadministration of a high-protein diet with SYNB1020 resulted in a dose-dependent reduction in circulating ammonia compared to mice receiving a high-protein diet with heat-killed SYNB1020 (Fig. 2A). The lowering of blood ammonia by SYNB1020 was associated with an increase in survival, as 100% of animals that received the highest doses of SYNB1020 survived the 24-hour testing period, whereas only 40 to 55% of mice survived when ammonia concentrations remained elevated. More chronic (up to 9 days) treatment of OTC $spf^{ash}$ mice with $SYNB1020^{KR}$ similarly normalized circulating ammonia concentrations after cotreatment with a high-protein diet (Fig. 2B, top), as compared to vehicle or to the non-arginine–producing control strain $EcN^{\Delta argR\Delta thyA}$, suggesting that the effects of SYNB1020 on ammonia lowering were sustained and driven by the engineered ammonia-arginine pathway. This ammonia normalization resulted in an improved survival during chronic administration of a high-protein diet over an engineered but non-arginine–producing strain, $EcN^{\Delta argR\Delta thyA}$, or vehicle high-protein control (Fig. 2B, bottom). We next examined the effects of SYNB1020 in a model of HE by rendering mice hyperammonemic with intraperitoneal treatment with the hepatotoxin thioacetamide (TAA). After 3 weeks of TAA administration, we observed an elevation in circulating ammonia concentrations compared to mice subjected to vehicle treatment (Fig. 2C). Administration of SYNB1020 to TAA-treated mice significantly decreased circulating ammonia concentrations compared to those observed in vehicle-treated or EcN-treated mice ($P = 0.0030$ and $P = 0.0214$, respectively; Fig. 2C). Although this study was not designed to assess mortality, we observed that in the vehicle/TAA group, one animal was found dead, one animal had to be euthanized because of poor body condition, and four of the remaining eight animals had to be sacrificed because of body weight loss. No animals were found dead, moribund, or had to be euthanized for

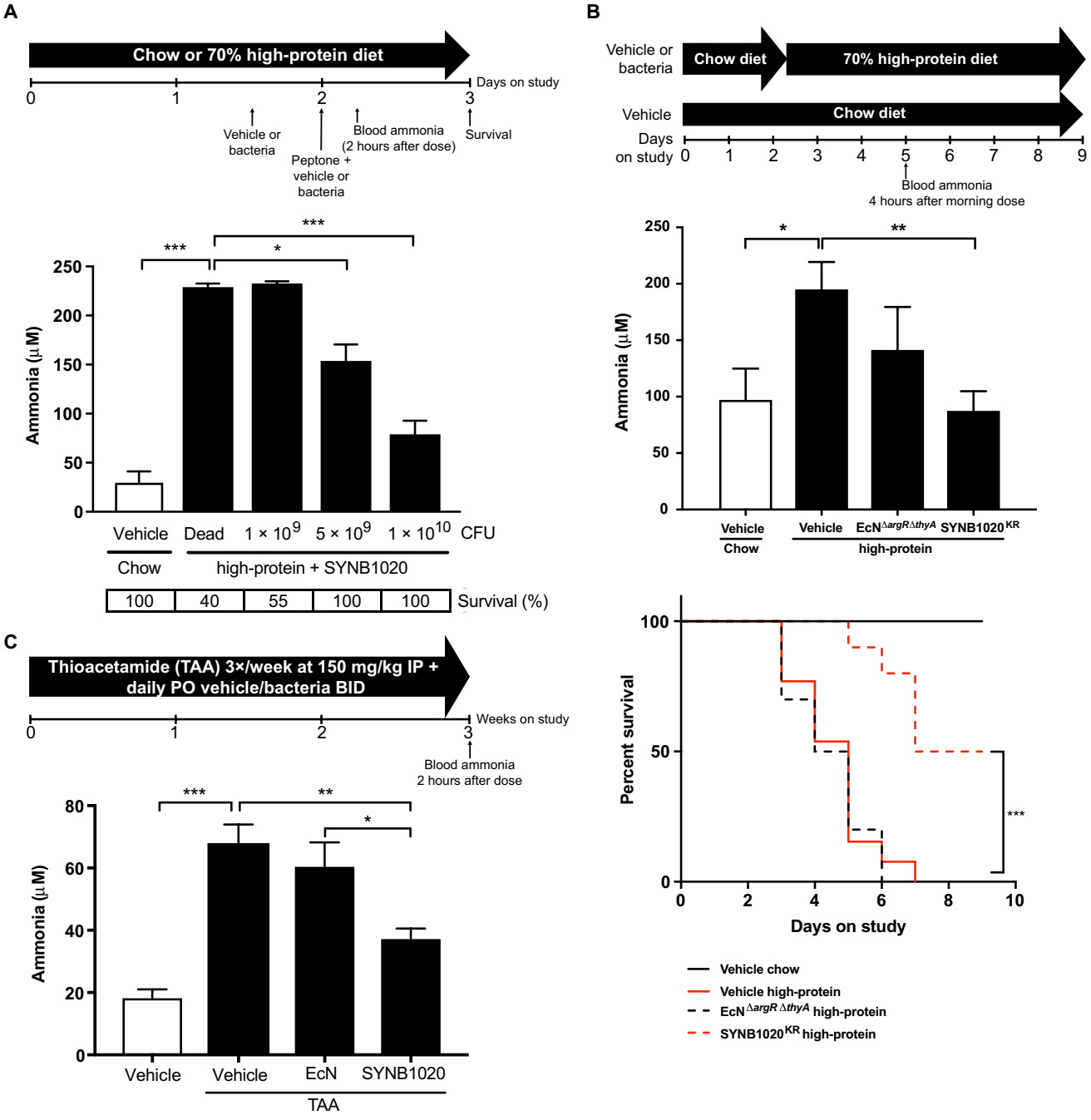


**Fig. 2. In vivo activity of engineered strains.** (**A**) Blood ammonia and percent survival in OTC$^{spf\text{-}ash}$ mice receiving normal chow or high-protein diet and dosed orally (PO) with vehicle [15% glycerol in phosphate-buffered saline (PBS)], heat-killed SYNB1020 (dead) or $1 \times 10^9$, $5 \times 10^9$, or $1 \times 10^{10}$ colony-forming units (CFU) of SYNB1020 ($n = 5$ vehicle/chow, $n = 5$ SYNB1020 dead/high protein, and $n = 9$ per group for all other groups). Statistical analysis comparing chow/vehicle with high-protein/SYNB1020 dead was performed using unpaired Student's $t$ test. Statistical analysis comparing high-protein/SYNB1020 dead with high-protein/SYNB1020$^{KR}$ was performed using one-way ANOVA on ranks, followed by Dunnett's multiple comparison test. (**B**) Top: Blood ammonia concentrations in OTC $spf^{ash}$ mice receiving normal chow or high-protein diet and dosed PO with vehicle ($H_2O$), EcN$^{\Delta argR\Delta thyA}$ ($1 \times 10^{10}$ CFU) or SYNB1020$^{KR}$ ($1 \times 10^{10}$ CFU) for 9 days ($n = 5$ vehicle/chow, $n = 10$ vehicle/high-protein, $n = 7$ EcN$^{\Delta argR\Delta thyA}$, and $n = 10$ SYNB1020$^{KR}$). Statistical analysis comparing chow/vehicle with high-protein/vehicle was performed using unpaired Student's $t$ test. Statistical analysis comparing high-protein/vehicle with high-protein/EcN$^{\Delta argR\Delta thyA}$ or SYNB1020 $^{KR}$ was performed using one-way ANOVA, followed by Dunnett's multiple comparison test. Bottom: Survival of OTC $spf^{ash}$ mice receiving normal chow or high-protein diet and dosed PO with vehicle, EcN$^{\Delta argR\Delta thyA}$ or SYNB1020$^{KR}$ for 9 days. Statistical analysis was performed using a $\log_l$-rank (Mantel-Cox) test. (**C**) Blood ammonia in Balb/cJ mice intraperitoneally (IP) dosed with or without TAA (150 mg/kg) in combination with vehicle (15% glycerol in PBS), were dosed PO with EcN ($1 \times 10^{10}$ CFU), or SYNB1020 ($1 \times 10^{10}$ CFU) for 3 weeks. Blood ammonia was measured on the last day of the experiment ($n = 10$ per group for vehicle, EcN/TAA, and SYNB1020/TAA and $n = 9$ for vehicle/TAA). Statistical analysis comparing vehicle with TAA/vehicle was performed using unpaired Student's $t$ test with Welch's correction. Statistical analysis comparing TAA/vehicle with TAA/EcN or TAA/SYNB1020 was performed using one-way ANOVA, followed by Tukey's multiple comparison test. Data are presented as means ± SEM. Statistical significance indicated as $^*P < 0.05$, $^{**}P < 0.01$, and $^{***}P < 0.0001$.

weight loss in the vehicle control, EcN/TAA, or SYNB1020/TAA groups. At the end of the study, the overall body weight change was +3.1 ± 1.1% in vehicle controls [$P < 0.0001$ versus vehicle/TAA, one-way analysis of variance (ANOVA) with Dunnett's multiple comparison test], −21.1 ± 2.7% in vehicle/TAA, −12.0 ± 1.7% in EcN/TAA ($P = 0.0023$ versus vehicle/TAA, one-way ANOVA with Dunnett's multiple comparison test), and −8.2 ± 1.8% in SYNB1020/TAA ($P < 0.0001$ versus vehicle/TAA, one-way ANOVA with Dunnett's multiple comparison test). No significant difference in body weight loss was observed between EcN/TAA and SYNB1020/TAA treatments ($P = 0.1251$, unpaired $t$ test with Welch's correction).

### SYNB1020 is well tolerated in mice and monkeys and is not found in tissues outside the GI tract

We evaluated SYNB1020 and the related strain SYNB1020$^{KR}$ for safety and persistence in male and female CD1 mice orally administered [twice daily (BID)] with SYNB1020, up to $7.8 \times 10^{10}$ CFU per dose, for 28 days with a 14-day recovery period and in male and female cynomolgus monkeys orally administered SYNB1020$^{KR}$ once daily at doses up to $1 \times 10^{12}$ for 28 days. In both studies, no treatment-related effects were observed on any parameters, including clinical signs, body weight, or food consumption, hematology, serum chemistry, organ weights, or histopathology (table S6).

We assessed the biodistribution of SYNB1020 in select tissues (spleen, liver, urinary bladder, and gonads) by quantitative polymerase chain reaction (qPCR) in the mouse study (table S7). SYNB1020 DNA was not detectable in any non-GI tissue sample from mice euthanized on day 29 (table S7), indicating no detectable translocation of SYNB1020 to the organs outside the GI tract.

The fecal excretion of SYNB1020 was directly evaluated in mice from this study using a qPCR method to specifically quantify SYNB1020 DNA. SYNB1020 DNA was present at high concentrations in the fecal samples of male and female mice dosed with either $5 \times 10^9$ or $1.5 \times 10^{11}$ CFU on days 7, 14, 21, and 28. Generally, SYNB1020 DNA concentrations in feces were dose related, being higher in the fecal samples from the $1.5 \times 10^{11}$ group than the $5 \times 10^9$ group. All SYNB1020 DNA concentrations were below the lower limit of quantification (LLOQ; <10 copies of SYNB1020 DNA/5 ng of stool DNA) in all groups on days 35 and 40 (Fig. 3, A and B). Similarly, after daily repeated oral gavage dose administration of the related strain SYNB1020$^{KR}$ to female cynomolgus monkeys, SYNB1020$^{KR}$ demonstrated clearance within 7 days of the last dose [as previously reported (*40*)].

### SYNB1020 is well tolerated, results in elevated nitrate in plasma and urine, and is excreted in feces as metabolically active cells in healthy volunteers

We studied the safety and tolerability of SYNB1020 in healthy volunteers in a first-in-human randomized, placebo-controlled, double-blinded phase 1 single-ascending dose (SAD) and multiple-ascending dose (MAD) study (study design shown in fig. S5). Fifty-two volunteers were enrolled and randomized to SYNB1020 or placebo. During the SAD study, 28 volunteers were enrolled across seven escalating dose cohorts, with treatment for a single day (21 volunteers dosed with SYNB1020 and 7 volunteers dosed with placebo). During the MAD study, 24 volunteers were enrolled across three escalating dose cohorts with treatment lasting for 14 days (18 volunteers dosed with SYNB1020 and 6 volunteers dosed with placebo). Baseline demographics for the study population are shown in table S8. No deaths or serious adverse events were reported in the study. Doses of SYNB1020 at or below $5 \times 10^{11}$ CFU (total daily dose, $1.5 \times 10^{12}$ CFU) were well tolerated by healthy volunteers. Higher doses were associated with mild-to-moderate GI adverse events. In the SAD study, three volunteers discontinued dosing due to mild-to-moderate nausea and vomiting [two volunteers in the $2 \times 10^{12}$ CFU three times daily (TID) cohort and one volunteer in the $1 \times 10^{12}$ CFU TID cohort], as did one volunteer in the highest MAD cohort ($5 \times 10^{11}$ CFU TID). Any adverse event leading to discontinuation occurred after the first dose (Table 2). No apparent signs of systemic toxicity were observed, and no apparent changes from baseline in C-reactive protein (fig. S6), in systolic or diastolic blood pressure, and in heart rate (figs. S7 and S8) or electrocardiogram (ECG) parameters, including QT interval (table S9) were observed.

We evaluated venous ammonia concentrations for 24-hour periods at baseline on day 2 and at day 13 after dose. Baseline fasting venous ammonia ranged from 11 to 59 μM (means ± SD, 28.8 ± 8.8 μM; local laboratory upper limit of normal, 32 μM) in healthy volunteers. As expected for healthy volunteers, physiological levels of ammonia were tightly controlled through the urea cycle, and no diurnal variation in venous ammonia ($P = 0.73$; Fig. 4A) or changes in 24-hour area under the curve (AUC) were observed in the ammonia profiles after the administration of SYNB1020 (Fig. 4B).

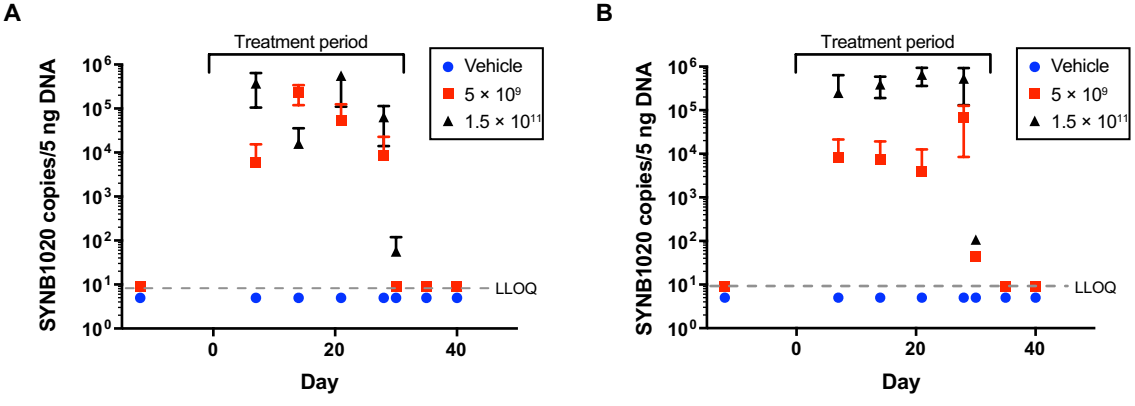


**Fig. 3. SYNB1020 excretion profile.** SYNB1020 excretion profile in (**A**) female ($n = 16$ per group) or (**B**) male ($n = 16$ per group) CD1 mice dosed with vehicle, $5 \times 10^9$ or $1.5 \times 10^{11}$ CFU SYNB1020 for 28 days. Fecal pellets were sterilely collected and analyzed for the presence of SYNB1020 DNA by qPCR using a validated method with a LLOQ of 10 copies/5 ng of DNA.

**Table 2. Treatment-emergent adverse events.** Adverse events reported by healthy volunteers dosed for either a single or multiple (14 days) days of dosing with SYNB1020. All reported adverse events were of mild or moderate severity. QD, once daily; TEAE, treatment-emergent adverse event.

| System organ class preferred term | Single-day cohorts | | | | | | | Multiple-day cohorts | | | Pooled placebo cohorts | |
|---|---|---|---|---|---|---|---|---|---|---|---|---|
| | $2 \times 10^9$ CFU QD (*N* = 3) *n* (%) | $2 \times 10^{10}$ CFU QD (*N* = 3) *n* (%) | $2 \times 10^{11}$ CFU QD (*N* = 3) *n* (%) | $2 \times 10^{12}$ CFU QD (*N* = 3) *n* (%) | $5 \times 10^{11}$ CFU TID (*N* = 3) *n* (%) | $1 \times 10^{12}$ CFU TID (*N* = 3) *n* (%) | $2 \times 10^{12}$ CFU TID (*N* = 3) *n* (%) | $2 \times 10^9$ CFU TID (*N* = 6) *n* (%) | $2 \times 10^{11}$ CFU TID (*N* = 6) *n* (%) | $5 \times 10^{11}$ CFU TID (*N* = 6) *n* (%) | SAD part (*N* = 7) *n* (%) | MAD part (*N* = 6) *n* (%) |
| Any TEAE | 0 | 0 | 0 | 2 (67) | 1 (33) | 1 (33) | 2 (67) | 0 | 5 (83) | 2 (33) | 0 | 1 (17) |
| GI disorders | 0 | 0 | 0 | 2 (67) | 0 | 1 (33) | 2 (67) | 0 | 3 (50) | 2 (33) | 0 | 1 (17) |
| Nausea | 0 | 0 | 0 | 1 (33) | 0 | 1 (33) | 2 (67) | 0 | 2 (33) | 2 (33) | 0 | 0 |
| Abdominal pain | 0 | 0 | 0 | 1 (33) | 0 | 0 | 0 | 0 | 2 (33) | 1 (17) | 0 | 0 |
| Vomiting | 0 | 0 | 0 | 0 | 0 | 1 (33) | 2 (67) | 0 | 0 | 1 (17) | 0 | 0 |
| Abdominal discomfort | 0 | 0 | 0 | 0 | 0 | 0 | 0 | 0 | 1 (17) | 1 (17) | 0 | 0 |
| Abdominal distension | 0 | 0 | 0 | 1 (33) | 0 | 0 | 0 | 0 | 0 | 0 | 0 | 0 |
| Diarrhea | 0 | 0 | 0 | 0 | 0 | 0 | 0 | 0 | 0 | 1 (17) | 0 | 0 |
| Flatulence | 0 | 0 | 0 | 0 | 0 | 0 | 0 | 0 | 0 | 0 | 0 | 1 (17) |
| General disorders and administration site conditions | 0 | 0 | 0 | 2 (67) | 0 | 0 | 0 | 0 | 2 (33) | 1 (17) | 0 | 1 (17) |
| Catheter site swelling | 0 | 0 | 0 | 2 (67) | 0 | 0 | 0 | 0 | 0 | 0 | 0 | 1 (17) |
| Vessel puncture site pain | 0 | 0 | 0 | 1 (33) | 0 | 0 | 0 | 0 | 0 | 1 (17) | 0 | 0 |
| Catheter site bruise | 0 | 0 | 0 | 0 | 0 | 0 | 0 | 0 | 1 (17) | 0 | 0 | 0 |
| Catheter site pain | 0 | 0 | 0 | 1 (33) | 0 | 0 | 0 | 0 | 0 | 0 | 0 | 0 |
| Vessel puncture site bruise | 0 | 0 | 0 | 0 | 0 | 0 | 0 | 0 | 1 (17) | 0 | 0 | 0 |
| Infections and infestations | 0 | 0 | 0 | 0 | 1 (33) | 0 | 0 | 0 | 0 | 0 | 0 | 0 |
| Upper respiratory tract infection | 0 | 0 | 0 | 0 | 1 (33) | 0 | 0 | 0 | 0 | 0 | 0 | 0 |
| Nervous system disorders | 0 | 0 | 0 | 0 | 0 | 0 | 0 | 0 | 0 | 1 (17) | 0 | 0 |
| Headache | 0 | 0 | 0 | 0 | 0 | 0 | 0 | 0 | 0 | 1 (17) | 0 | 0 |

In healthy volunteers, we observed no apparent change from baseline in blood urea nitrogen, arginine, citrulline, 24-hour urinary urea and nitrogen, or urinary orotic acid (table S10). However, an increase in urinary nitrate was seen (Fig. 4C). Furthermore, when volunteers were dosed orally with oral $^{15}$N-ammonium chloride ($^{15}NH_4Cl$; 20 mg/kg) during treatment with SYNB1020, we observed an increase from baseline in plasma $^{15}$N-nitrate and urinary $^{15}$N-nitrate [means (90% confidence interval), 1160 (955 to 1370) mole percent excess (MPE)·ml] in the $5 \times 10^{11}$ CFU SYNB1020 TID treatment group, but not in the placebo group (Fig. 4, D and E). The increase in $^{15}$N-nitrate was dose responsive. We observed no change from baseline in urinary or plasma $^{15}$N-urea or plasma $^{15}$N-citrulline (table S11). SYNB1020 was detected by strain-specific qPCR in the feces of all volunteers in the treatment groups but none of the placebo volunteers, and the maximum qPCR copy number increased in a dose-dependent manner (Fig. 5A). Steady-state levels of SYNB1020 DNA in feces were reached by 2 days based on visual estimation. The mean residence time after cessation of dosing was 48 hours. There was no evidence of colonization because SYNB1020 was below the limit of detection in feces within 2 weeks of the last dose (Fig. 5B). We also confirmed that SYNB1020 excreted in stool was alive and metabolically active. Because SYNB1020 does not contain a

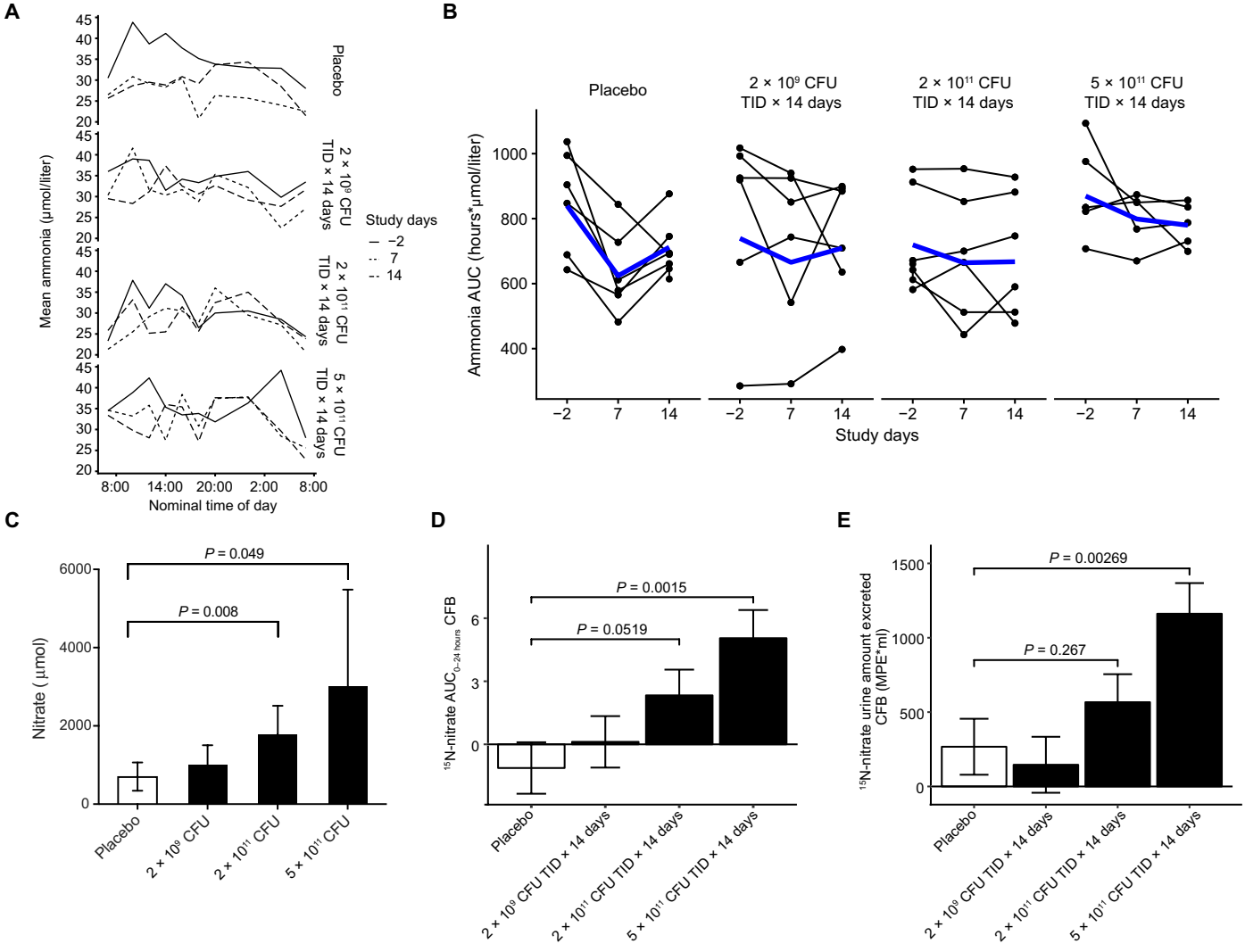


**Fig. 4. Evaluation of SYNB1020 safety and pharmacodynamics in healthy volunteers receiving 14 days of dosing with SYNB1020 or placebo.** (**A**) Diurnal mean plasma ammonia levels measured over 24 hours across MAD cohorts of healthy volunteers treated with placebo ($n = 6$), $2 \times 10^9$ CFU TID ($n = 6$), $2 \times 10^{11}$ CFU TID ($n = 6$), or $5 \times 10^{11}$ CFU TID ($n = 5$). (**B**) Individual 24-hour plasma AUC ammonia concentrations in MAD cohorts treated with placebo ($n = 6$), $2 \times 10^9$ CFU TID ($n = 6$), $2 \times 10^{11}$ CFU TID ($n = 6$), or $5 \times 10^{11}$ CFU TID ($n = 5$). Individual volunteers are shown as black lines. Mean ammonia AUC per cohort is depicted in blue. (**C**) Urinary nitrate concentrations were measured 24 hours after dose in MAD cohorts by a colorimetric method in MAD cohorts treated with placebo ($n = 6$), $2 \times 10^9$ CFU TID ($n = 6$), $2 \times 10^{11}$ CFU TID ($n = 6$), or $5 \times 10^{11}$ CFU TID ($n = 5$). Nitrate concentration was multiplied by the total urine volume to obtain total nitrate in micromole. (**D**) Mean plasma AUC (0 to 24 hours) $^{15}$N-nitrate change from baseline (CFB) after oral administration of $^{15}$N-$NH_3$Cl in MAD cohorts treated with placebo ($n = 6$), $2 \times 10^9$ CFU TID ($n = 6$), $2 \times 10^{11}$ CFU TID ($n = 6$), or $5 \times 10^{11}$ CFU TID ($n = 5$). (**E**) Total $^{15}$N-urinary nitrate change from baseline after oral administration of $^{15}$N-$NH_3$Cl in MAD cohorts treated with placebo ($n = 6$), $2 \times 10^9$ CFU TID ($n = 6$), $2 \times 10^{11}$ CFU TID ($n = 6$), or $5 \times 10^{11}$ CFU TID ($n = 5$).

selectable marker for confirmation of live bacteria, we instead demonstrated the activity of SYNB1020 present in fecal samples by measuring the arginine biosynthetic activity in human stool after introducing $^{15}$N-$NH_3$ into the stool homogenate and then quantifying the amount of $^{15}$N-arginine produced. $^{15}$N-arginine production was observed in stool samples from untreated healthy volunteers inoculated with increasing SYNB1020 CFU (Fig. 5C) and from volunteers treated orally with SYNB1020 for 14 days, but not from predose stool samples or from placebo control stool samples (Fig. 5D). These studies show that SYNB1020 cells were viable and metabolically active in feces after passage through the GI tract of healthy humans.

## DISCUSSION

We demonstrated the design, characterization, and translational development of SYNB1020 as a clinical candidate for the treatment of hyperammonemia. Although several engineered bacteria and probiotic strains have been created and tested in preclinical models (*61*), few have progressed into clinical development. An engineered *Lactococcus lactis* strain producing interleukin-10 has been evaluated clinically for the treatment of inflammatory bowel disease (*62*), and a *L. lactis* strain producing trefoil factors has been studied for the treatment of oral mucositis (*63*). Some studies with *Listeria monocytogenes* strains engineered as vaccines for various cancers have also been evaluated (*64*). However, published data describing

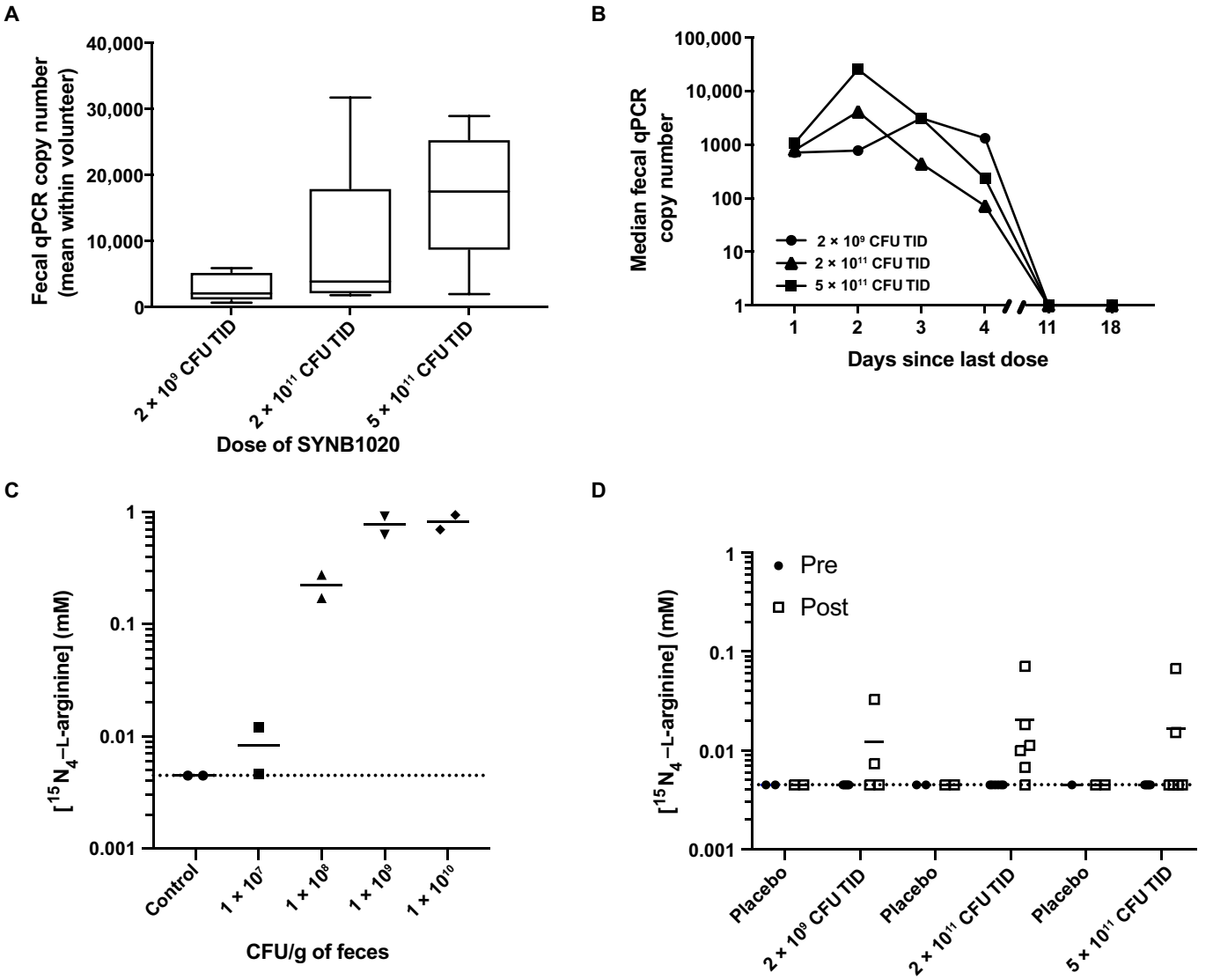


**Fig. 5. SYNB1020 excretion profile and activity in stool from healthy volunteers.** Groups of eight volunteers per cohort (six SYNB1020 and two placebo) were enrolled and dosed with either placebo ($n = 6$) or SYNB1020 at $2 \times 10^9$ CFU TID ($n = 6$), $2 \times 10^{11}$ CFU TID ($n = 6$), or $5 \times 10^{11}$ CFU TID ($n = 5$). (**A**) Steady-state concentrations of SYNB1020 DNA in feces of healthy volunteers dosed for 14 days. (**B**) Clearance of SYNB1020 DNA from volunteers' stool after dosing using qPCR (LLOQ, 10 copies/5 ng of DNA). (**C**) $^{15}N_4$–L-arg production after normal stool ($n = 2$ per group) was spiked with $^{15}N$-$NH_3$ and increasing doses of SYNB1020. (**D**) Stool from healthy volunteers dosed with placebo (black circles; $n = 2$ per group) or SYNB1020 (open squares; $n = 6$ per group) was inoculated with $^{15}N$-$NH_3$, and $^{15}N_4$–L-arg was measured.

the preclinical and translational characterization of the drug-like properties of these strains, including safety, exposure, excretion profile, dose response, and biomarkers demonstrating strain activity in humans are limited.

We modified the genome of EcN to substantially enhance ammonia consumption through the increased production of arginine over the wild-type strain. We showed that, in contrast to previous engineered arginine-producing *E. coli* strains (*36*), adding a feedback-resistant version of *N*-acetylglutamate synthase (*argA*) under control of FNR and deleting the arginine repressor gene (*argR*) had a substantial effect on gene expression when cultured anaerobically, with the modified strain exhibiting increased expression of the full arginine biosynthetic pathway and decreased expression of genes involved in arginine catabolism. Concentrations of arginine produced by SYNB1020 (and extrapolated to human production over 24 hours) are expected to be <12 mg/kg per day, well below amounts used as dietary supplements, and are thus are expected to be safe (*46*).

The design of SYNB1020 also included a feature to limit its replication, the deletion of *thyA*, rendering the strain a thymidine auxotroph. Our transcriptomic analysis of $EcN^{\Delta thyA}$ revealed that deletion of *thyA* had a profound effect on the overall state of the bacterial cell, even in the presence of exogenous thymidine, resulting in transcriptional signatures of cellular stress. A signal of stress response in the presence of thymidine may reflect either the need to transport exogenous thymidine into the cell or the requirement to convert thymidine to deoxythymidine monophosphate, a reaction that consumes adenosine 5′-triphosphate (*65*). This stress may also present an adaptive pressure on engineered EcN. However,

implementation of this biocontainment strategy prevented replication of the cells in the absence of exogenous thymidine and is therefore unlikely to result in genetic drift in vivo. The *thyA* deletion did not impair expression of the arginine biosynthesis pathway in vitro. Whereas the strain does show the expression of stress response genes even in the presence of exogenous thymidine, growth of the strain during manufacturing (with thymidine supplementation) occurred at a rate that was indistinguishable from that of a nondeletion strain. Hence, there is no anticipated adaptive pressure for mutants to arise during manufacturing, and we have failed to isolate any variants from our manufacturing efforts that are capable of growth in the absence of thymidine supplementation. Consequently, we interpret the expression of stress response genes to reflect the fact that thymidine supplementation of a *thyA* deletion strain is not physiologically identical to endogenous thymidine production in a $thyA^+$ strain but does not necessarily signal that the deletion strain is compromised for its ability to grow and replicate at a healthy rate. These observations underscore the importance of studying the global impacts of auxotrophy strategies on the physiology of engineered strains.

SYNB1020 demonstrated dose-dependent lowering of plasma ammonia and improved survival in OTC $spf^{ash}$ mice. The OTC $spf^{ash}$ mouse model carries a splicing mutation in the gene encoding OTC, one of the most common genetic loci associated with human UCDs (*60*, *66*). Hyperammonemia can induce cerebral edema, energy failure, neurotransmitter alterations, reactive oxygen species, or inflammation (*67*, *68*), and although we did not directly explore these mechanisms in this study, it is possible that SYNB1020 and $SYNB1020^{KR}$ enhanced survival by decreasing these ammonia-induced effects. We also used the TAA-based hepatic injury model in wild-type Balb/c mice, an accepted preclinical model of HE, as a second model of systemic hyperammonemia (*69*). In both mouse models, a dose of $5 \times 10^9$ to $1 \times 10^{10}$ CFU was efficacious in lowering ammonia. However, projection of a suitable human dose for gut-based therapies from preclinical models is challenging due to differences in GI physiology, substrate concentration, and metabolism. Probiotics, including VSL#3 and EcN, have previously been shown to have beneficial effects in cirrhotic patients. It has been reported that fasting ammonia levels were decreased in cirrhotic patients treated with probiotic VSL#3, whereas ammonia increased in patients receiving placebo (*70*). In addition, reductions in venous ammonia levels were reported after 30 days of synbiotic supplementation compared to presupplementation values in cirrhotic patients (*71*). EcN has been reported to have antimicrobial and anti-inflammatory/immunomodulatory effects as well as direct restorative effects on gut epithelium and permeability (*72*, *73*). In our studies, we observed that the non-arginine–producing strains EcN and $EcN^{\Delta argR \Delta thyA}$ caused no statistically significant ammonia lowering in both models tested and no notable improvement in survival in OTC $spf^{ash}$ mice, suggesting that the efficacy observed with $SYNB1020^{KR}$ is driven by the engineered ammonia-arginine pathway. The efficacious human dose will be further explored clinically in patients with hyperammonemia.

SYNB1020 was advanced to human testing in a SAD/MAD trial in healthy adult male and female volunteers and found to be safe and well tolerated at dose concentrations up to $5 \times 10^{11}$ CFU TID for 14 days, with no systemic toxicities of infections observed. Nausea and vomiting at the highest doses (single and multiple doses of $2 \times 10^{12}$ CFU and one subject administered $5 \times 10^{11}$ CFU) were observed and have been reported in clinical trials for other microbiome-based treatments delivered to the upper intestinal tract (*72*, *74*, *75*). EcN (Mutaflor) has been well tolerated in adult and pediatric patients, with the most common side effect being flatulence (*72*); however, commercial doses of Mutaflor are lower ($2.5 \times 10^9$ to $2.5 \times 10^{10}$ CFU per dose) than the concentrations explored in this study ($2.0 \times 10^9$ to $2.0 \times 10^{12}$ CFU per dose). Because of the short duration of this study and the nonreplicative nature of the SYNB1020 strain, we did not evaluate the effect of chronic dosing with SYNB1020 on the microbiome. Future human studies with longer-term dosing may be more appropriate to evaluate these changes. This study was not designed to detect any change in ammonia in healthy individuals whose physiological concentrations are tightly controlled. Arginine can be metabolized by nitric oxide synthase, resulting in production of nitric oxide and citrulline (*78*), and ultimately excretion of nitrate in urine. A dose-dependent elevation in concentrations of urinary nitrate and plasma and urinary $^{15}$N-nitrate was observed in healthy volunteers dosed with SYNB1020, making nitrate a potential indicator of strain activity in humans. Although we were able to detect urinary nitrates in mice and monkeys in some studies, we did not consistently and reliably observe elevations of this marker (or other arginine-related metabolites) with our bacteria in preclinical species, which could be potentially explained by differences in diet, microbiota composition, and/or gut-residence time between animals and humans.

Traditional pharmacokinetic measures are not applicable in gut-based therapies because the bacteria are not systemically absorbed, and thus, blood concentrations cannot be measured. To follow the exposure and excretion profile of SYNB1020, we used a sensitive and specific qPCR method to detect the bacteria in fecal samples collected from mice, monkeys, and humans. This tool allowed us to establish a dose response for SYNB1020 and an excretion profile through demonstration of presence of SYNB1020 in feces. Establishing that SYNB1020 was not detectable in tissues outside the GI tract was also a valuable preclinical use of this tool. EcN can improve intestinal barrier function (*75*) and is used in chronic treatment of inflammatory bowel disease where barrier function may be compromised (*41*–*44*). In the TAA model, which has increased intestinal permeability, we found reduced uptake of orally delivered fluorescein isothiocyanate–labeled dextran, a marker of intestinal permeability (*76*). These observations will be supported by further study of the safety of engineered EcN strains in chronic disease models and patients.

Limitations of this study include the inability to detect a quantitative biomarker of arginine production in preclinical species or humans and the inability to define a likely therapeutic dose range in patients with metabolic disease. A quantitative biomarker or indicator of strain activity could provide a means of dose extrapolation between preclinical species and humans and between healthy volunteers and patients. Our inability to detect such a biomarker may be due to the complex and rapid metabolism of arginine to a large number of products such as ornithine, citrulline, nitric oxide (further oxidized to nitrate and excreted in urine), urea, creatine, agmatine, polyamines, proline, and others (*77*). In addition, arginine metabolism is heavily compartmentalized between various organs including the liver, kidneys, intestine, and vascular endothelium (*77*), adding another layer of complexity. However, a previous study, using a $^{15}$N-arginine tracer, has shown that ~60% of orally delivered arginine is metabolized to urea in humans, a conversion mostly attributed to intestinal arginase activity (*78*). Therefore, most of $NH_3$

converted to arginine by SYNB1020 might be excreted in the form of urinary urea. Unfortunately, the amount of urea excreted in urine at baseline was too large and variable for us to detect reliable quantitative changes in urea excretion after SYNB1020 treatment in our preclinical model or clinical study. Unlike urea, the excretion of nitrate in urine accounts for a much smaller fraction of dietary arginine, ranging from 0.07 to 0.4% depending on the route of administration (oral or intragastric) (*79*, *80*), and the proportion of urinary nitrate originating from dietary arginine is substantial (*80*). Although elevation in plasma and urinary nitrate is a potential qualitative indicator of arginine metabolism related to strain activity, it may not be a quantitative marker for arginine given the alternative mechanisms of elimination of arginine described above.

On the basis of the preclinical activity of SYNB1020 and its safety and tolerability in humans, we propose that this strain should be further evaluated in conditions of hyperammonemia including UCD and HE. SYNB1020 is currently being evaluated in a phase 2a study in patients with cirrhosis (ClinicalTrials.gov, identifier: NCT03447730).

## MATERIALS AND METHODS

### Study design

In this study, we engineered the probiotic bacterium EcN to create the strain SYNB1020, which consumes ammonia in its environment and converts it to arginine. The endogenous arginine biosynthetic pathway was modified in this strain to remove natural feedback repression from arginine and to induce expression of arginine biosynthetic genes under control of an anaerobic promoter. The strain was tested in vitro for ammonia consumption and arginine production and metabolism, and safety was evaluated in two mouse models of hyperammonemia. The tolerability, biodistribution, and pharmacokinetics of the strain were tested in female cynomolgus monkeys. The strain was also tested in humans for safety, tolerability, and production of metabolites of arginine. All procedures performed on animals were in accordance with the humane guidelines for ethical and sensitive care by the Institutional Animal Care and Use Committee (IACUC) of the U.S. National Institutes of Health.

#### *Mouse studies*

The objectives of the studies conducted in mice were to demonstrate the exposure of orally administered bacteria to the intestinal tract and to measure the efficacy in two preclinical models of hyperammonemia. Studies were conducted in models of hyperammonemia, including the OTC $spf^{ash}$ and TAA mice. In these studies, the effects of SYNB1020 and related arginine-producing strains were compared to unengineered EcN or heat-killed SYNB1020 (Fig. 2, A to D). The excretion profile of SYNB1020 was evaluated in mice after 28 days of oral treatment with SYNB1020 (Fig. 3).

#### *Repeat-dose tolerability and pharmacokinetic study in female cynomolgus monkeys*

The methods for these studies have been previously described (*40*). The animals were group-housed in temperature- and humidity-controlled environments in cages that complied with the Animal Welfare Act. They were offered PMI's LabDiet Fiber-Plus Monkey Diet 5049 biscuits BID and provided fresh drinking water ad libitum. Animals were given fruits, vegetables, other dietary supplements, and cage enrichment devices throughout the course of the study according to the facility standard operating procedures. Animals were fasted for at least 2 hours before dose administration and fed within 1 hour after dose. Briefly, $SYNB1020^{KR}$ and $EcN^{KR}$ dosing formulations were prepared daily from frozen stocks and were dosed via nasogastric tube to three females per group once daily for 28 days at levels of 0 (PBS buffer), $1 \times 10^9$, and $1 \times 10^{12}$ CFU per animal. In-life assessments included daily clinical observations and weekly body weights. Blood samples were collected for clinical pathology assessment before the initial dose and on days 2, 14, and 30. Samples for fecal analysis for the presence of $SYNB1020^{KR}$ or $EcN^{KR}$ were also collected twice weekly during the study and after dose for an additional 7 days. No terminal necropsies were performed, and animals were returned to the stock colony at the end of the recovery period.

These studies were conducted in a facility accredited by the Association for Assessment and Accreditation of Laboratory Animal Care that has an Animal Welfare Assurance issued by the Office of Laboratory Animal Welfare and is registered with the U.S. Department of Agriculture. The study was reviewed and approved by IACUC responsible for compliance with applicable laws and regulations concerning the humane care and use of laboratory animals.

#### *Clinical study in healthy human volunteers*

A phase 1, randomized, double-blinded, placebo-controlled, dose-escalating study (NCT03179878) evaluated SYNB1020 in healthy volunteer male and female volunteers in the inpatient setting to evaluate safety and tolerability of SYNB1020 versus placebo (Fig. 4 and table S7). This study was conducted according to the provisions of the Declaration of Helsinki and its current amendments, and the International Conference on Harmonization Guidelines for Good Clinical Practice. All volunteers reviewed and signed informed consent forms approved by the institutional review board before initiation of study procedures. Both volunteers and investigators were blinded to randomized treatment group assignment. The primary objective was to evaluate the safety and tolerability of SYNB1020 after single and multiple doses in healthy volunteers. The end points related to this objective included the nature and frequency of adverse events, laboratory assessments (e.g., blood chemistry, complete blood count, and urinalysis), and ECGs. Secondary and exploratory objectives were assessment of GI tolerability, SYNB1020 kinetics in feces (measured with qualitative and qPCR fecal assays) after dosing, measurements of plasma ammonia (including 24-hour AUC), amino acids, and blood urea nitrogen; 24-hour urinary urea and nitrogen and urinary orotic acid; and fecal nitrogen. In addition, nitrogen metabolism was studied using stable isotope $^{15}NH_4Cl$ measuring urinary total $^{15}N$, $^{15}N$-urea (N1 and N2), $^{15}N$-nitrate, $^{15}N$-ammonia, plasma $^{15}N$-urea (N1 and N2), $^{15}N$-nitrate, and $^{15}N$-citrulline. The dosing and study design are shown in fig. S5. Volunteers were followed for safety and SYNB1020 clearance for up to 100 days after the last study dose.

This study was composed of adult (18 to 64 years) healthy male and female volunteers of nonchildbearing potential who had no acute or chronic medical, surgical, psychiatric, or social conditions or laboratory abnormalities that may have increased subject risk or confounded interpretation of study results. Prohibited medical conditions (current and/or past) comprised autoimmune disorders (including inflammatory or irritable bowel disorders), infectious diseases, active infections, hematemesis or hematochezia, diabetes mellitus, personal or family history of UCD, dependence on alcohol or drugs of abuse, or surgery or hospitalization within 6 months of screening.

### Statistical analysis

#### *Mouse studies*

Data are presented as means ± SEM. Statistical analysis was performed using Graphpad Prism software. Data were tested for normality before choosing the appropriate statistical test. The details of the tests used can be found in the figure legends. The criteria for statistical significance were set as $P < 0.05$; $P$ values shown refer to post hoc analysis.

#### *Clinical study*

Clinical per-protocol analyses were performed using the statistical software program, SAS, and post hoc assessments were performed in R (version 3.3 or greater). Descriptive statistics were calculated for most parameters. For $^{15}$N-nitrate AUC and urinary excretion, a linear mixed-effects model with a categorical fixed effect by treatment and random effect by subject was used to estimate the effect using the lme function in the nlme R package. Analyses, which were exploratory and for which the study was not adequately powered for multiplicity adjustments, have been summarized in supplementary tables with descriptive statistics.

## SUPPLEMENTARY MATERIALS

www.sciencetranslationalmedicine.org/cgi/content/full/11/475/eaau7975/DC1

Materials and Methods

Fig. S1. Demonstration of in vivo induction of the $P_{fnrS}$ using green fluorescent protein as a reporter in EcN strain.

Fig. S2. EcN strains lacking the *thyA* gene fail to grow in rich media lacking exogenous thymidine.

Fig. S3. Differential gene expression for SYNB1020 compared to EcN for genes in the L-arg biosynthesis pathway.

Fig. S4. Dose-dependent fecal excretion of EcN and SYNB1020 strains in mice.

Fig. S5. Study design of a randomized, double-blinded, placebo-controlled study to assess the safety, tolerability, and pharmacodynamics of SYNB1020 in healthy volunteers.

Fig. S6. Change from baseline in C-reactive protein.

Fig. S7. Time-matched change from baseline for diastolic blood pressure.

Fig. S8. Time-matched change from baseline for systolic blood pressure.

Table S1. Differential gene expression comparisons of SYNB1020 and EcN$^{\Delta thyA}$ to EcN in vitro.

Table S2. Quantification of viable SYNB1020$^{KR}$ in mouse cecolonic samples over time.

Table S3. Average ECN$^{StrR}$ or SYNB1020$^{KR}$ CFU recovered from GI contents of mice dosed with each strain.

Table S4. Activity rate of SYNB1020$^{KR}$ recovered from mouse cecum and colon.

Table S5. Arginine pathway metabolites in mouse and nonhuman primates.

Table S6. Clinical and laboratory results from a 28-day oral toxicity study of SYNB1020 in mice.

Table S7. Mice with detectable SYNB1020 DNA in tissues as measured by qPCR.

Table S8. Baseline demographics for the phase 1 study population.

Table S9. ECG QT interval in the phase 1, multiple-day, study population.

Table S10. Laboratory results for urea cycle products in the multiple-day cohort phase 1 study population.

Table S11. $^{15}$N metabolites in the phase 1 study population.

Table S12. Primers used to characterize SYNB1020 genetic modifications.

Table S13. Fermentation medium (FM1).

References (*81*–*90*)

## REFERENCES AND NOTES


1. D. T. Riglar, T. W. Giessen, M. Baym, S. J. Kerns, M. J. Niederhuber, R. T. Bronson, J. W. Kotula, G. K. Gerber, J. C. Way, P. A. Silver, Engineered bacteria can function in the mammalian gut long-term as live diagnostics of inflammation. *Nat. Biotechnol.* **35**, 653–658 (2017).
2. M. L. Hanson, J. A. Hixon, W. Li, B. K. Felber, M. R. Anver, C. A. Stewart, B. M. Janelsins, S. K. Datta, W. Shen, M. H. McLean, S. Durum, Oral delivery of IL27 recombinant bacteria attenuates immune colitis in mice. *Gastroenterology* **146**, 210–221.e13 (2014).
3. L. Steidler, W. Hans, L. Schotte, S. Neirynck, F. Obermeier, W. Falk, W. Fiers, E. Remaut, Treatment of murine colitis by *Lactococcus lactis* secreting interleukin-10. *Science* **289**, 1352–1355 (2000).
4. Z. Z. R. Hamady, N. Scott, M. D. Farrar, M. Wadhwa, P. Dilger, T. R. Whitehead, R. Thorpe, K. T. Holland, J. P. A. Lodge, S. R. Carding, Treatment of colitis with a commensal gut bacterium engineered to secrete human TGF-β1 under the control of dietary xylan 1. *Inflamm. Bowel Dis.* **17**, 1925–1935 (2011).
5. F. F. Duan, J. H. Liu, J. C. March, Engineered commensal bacteria reprogram intestinal cells into glucose-responsive insulin-secreting cells for the treatment of diabetes. *Diabetes* **64**, 1794–1803 (2015).
6. T.-C. D. Shen, L. Albenberg, K. Bittinger, C. Chehoud, Y.-Y. Chen, C. A. Judge, L. Chau, J. Ni, M. Sheng, A. Lin, B. J. Wilkins, E. L. Buza, J. D. Lewis, Y. Daikhin, I. Nissim, M. Yudkoff, F. D. Bushman, G. D. Wu, Engineering the gut microbiota to treat hyperammonemia. *J. Clin. Invest.* **125**, 2841–2850 (2015).
7. V. M. Isabella, B. N. Ha, M. J. Castillo, D. J. Lubkowicz, S. E. Rowe, Y. A. Millet, C. L. Anderson, N. Li, A. B. Fisher, K. A. West, P. J. Reeder, M. M. Momin, C. G. Bergeron, S. E. Guilmain, P. F. Miller, C. B. Kurtz, D. Falb, Development of a synthetic live bacterial therapeutic for the human metabolic disease phenylketonuria. *Nat. Biotechnol.* **36**, 857–864 (2018).
8. W. H. Tang, T. Kitai, S. L. Hazen, Gut microbiota in cardiovascular health and disease. *Circ. Res.* **120**, 1183–1196 (2017).
9. K. Yamashiro, R. Tanaka, T. Urabe, Y. Ueno, Y. Yamashiro, K. Nomoto, T. Takahashi, H. Tsuji, T. Asahara, N. Hattori, Gut dysbiosis is associated with metabolism and systemic inflammation in patients with ischemic stroke. *PLOS ONE* **12**, e0171521 (2017).
10. M. Imler, G. Chabrier, C. Simon, J. L. Schlienger, Intestinal ammonium production in the rat: The role of the colon, small intestine, and circulating glutamine. *Res. Exp. Med.* **188**, 1–7 (1988).
11. E. A. Phear, B. Ruebner, The in vitro production of ammonium and amines by intestinal bacteria in relation to nitrogen toxicity as a factor in hepatic coma. *Br. J. Exp. Pathol.* **37**, 253–262 (1956).
12. E. Wolpert, S. F. Phillips, W. H. J. Summerskill, Transport of urea and ammonia production in the human colon. *Lancet* **298**, 1387–1390 (1971).
13. E. B. Tapper, Z. G. Jiang, V. R. Patwardhan, Refining the ammonia hypothesis: A physiology-driven approach to the treatment of hepatic encephalopathy. *Mayo Clin. Proc.* **90**, 646–658 (2015).
14. J. T. Brosnan, Interorgan amino acid transport and its regulation. *J. Nutr.* **133**, 2068S–2072S (2003).
15. H. G. Windmueller, A. E. Spaeth, Uptake and metabolism of plasma glutamine by the small intestine. *J. Biol. Chem.* **249**, 5070–5079 (1974).
16. M. Walser, L. J. Bodenlos, Urea metabolism in man. *J. Clin. Invest.* **38**, 1617–1626 (1959).
17. H. L. Mobley, R. P. Hausinger, Microbial ureases: Significance, regulation, and molecular characterization. *Microbiol. Rev.* **53**, 85–108 (1989).
18. D. Häussinger, B. Stoll, T. Stehle, W. Gerok, Hepatocyte heterogeneity in glutamate metabolism and bidirectional transport in perfused rat liver. *Eur. J. Biochem.* **185**, 189–195 (1989).
19. D. Häussinger, W. Gerok, Hepatocyte heterogeneity in glutamate uptake by isolated perfused rat liver. *Eur. J. Biochem.* **136**, 421–425 (1983).
20. S. W. M. Olde Damink, R. Jalan, C. H. C. Dejong, Interorgan ammonia trafficking in liver disease. *Metab. Brain Dis.* **24**, 169–181 (2009).
21. J. V. Leonard, A. A. M. Morris, Urea cycle disorders. *Semin. Neonatol.* **7**, 27–35 (2002).
22. D. R. Aldridge, E. J. Tranah, D. L. Shawcross, Pathogenesis of hepatic encephalopathy: Role of ammonia and systemic inflammation. *J. Clin. Exp. Hepatol.* **5**, S7–S20 (2015).
23. D. Suraweera, V. Sundaram, S. Saab, Evaluation and management of hepatic encephalopathy: Current status and future directions. *Gut Liver* **10**, 509–519 (2016).
24. H. Vilstrup, P. Amodio, J. Bajaj, J. Cordoba, P. Ferenci, K. D. Mullen, K. Weissenborn, P. Wong, Hepatic encephalopathy in chronic liver disease: 2014 practice guideline by the American Association for the study of liver diseases and the European Association for the study of the liver. *Hepatology* **60**, 715–735 (2014).
25. S. Scaglione, S. Kliethermes, G. Cao, D. Shoham, R. Durazo, A. Luke, M. L. Volk, The epidemiology of cirrhosis in the United States: A population-based study. *J. Clin. Gastroenterol.* **49**, 690–696 (2015).
26. Y. Kim, A. Ejaz, A. Tayal, G. Spolverato, J. F. P. Bridges, R. A. Anders, T. M. Pawlik, Temporal trends in population-based death rates associated with chronic liver disease and liver cancer in the United States over the last 30 years. *Cancer* **120**, 3058–3065 (2014).
27. K. R. Patidar, J. S. Baja, Covert and overt hepatic encephalopathy: Diagnosis and management. *Clin. Gastroenterol. Hepatol.* **13**, 2048–2061 (2015).
28. J. O. Clemmesen, F. S. Larsen, J. Kondrup, B. A. Hansen, P. Ott, Cerebral herniation in patients with acute E liver failure is correlated with arterial ammonia concentration. *Hepatology* **29**, 648–653 (1999).
29. P. S. Ge, B. A. Runyon, Serum ammonia level for the evaluation of hepatic encephalopathy. *JAMA* **312**, 643–644 (2014).
30. J. P. Ong, A. Aggarwal, D. Krieger, K. A. Easley, M. T. Karafa, F. Van Lente, A. C. Arroliga, K. D. Mullen, Correlation between ammonia levels and the severity of hepatic encephalopathy. *Am. J. Med.* **114**, 188–193 (2003).
31. A. M. Dawson, J. McLaren, S. Sherlock, Neomycin in the treatment of hepatic coma. *Lancet* **273**, 1262–1268 (1957).
32. B. B. Fast, S. J. Wolfe, J. M. Stormont, C. S. Davidson, Antibiotic therapy in the management of hepatic coma. *A.M.A. Arch. Intern. Med.* **101**, 467–475 (1958).

33. C. L. H. van Berlo, P. A. M. van Leeuwen, P. B. Soeters, Porcine intestinal ammonia liberation: Influence of food intake, lactulose, and neomycin treatment. *J. Hepatol.* **7**, 250–257 (1988).
34. N. M. Bass, K. D. Mullen, A. Sanyal, F. Poordad, G. Neff, C. B. Leevy, S. Sigal, M. Y. Sheikh, K. Beavers, T. Frederick, L. Teperman, D. Hillebrand, S. Huang, K. Merchant, A. Shaw, E. Bortey, W. P. Forbes, Rifaximin treatment in hepatic encephalopathy. *N. Engl. J. Med.* **362**, 1071–1081 (2010).
35. C. R. Bosoi, C. Parent-Robitaille, K. Anderson, M. Tremblay, C. F. Rose, AST-120 (spherical carbon adsorbent) lowers ammonia levels and attenuates brain edema in bile duct-ligated rats. *Hepatology* **53**, 1995–2002 (2011).
36. B. S. Rajagopal, J. DePonte III, M. Tuchman, M. H. Malamy, Use of inducible feedback-resistant *N*-acetylglutamate synthetase (*argA*) genes for enhanced arginine biosynthesis by genetically engineered *Escherichia coli* K-12 strains. *Appl. Environ. Microbiol.* **64**, 1805–1811 (1998).
37. G. Neff, Factors affecting compliance and persistence with treatment for hepatic encephalopathy. *Pharmacotherapy* **30**, 22S–27S (2010).
38. S. L. Flamm, Considerations for the cost-effective management of hepatic encephalopathy. *Am. J. Manag. Care* **24**, S51–S61 (2018).
39. T. M. Wassenaar, Insights from 100 years of research with probiotic *E. coli*. *Eur. J. Microbiol. Immunol.* **6**, 147–161 (2016).
40. C. Kurtz, W. S. Denney, L. Blankstein, S. E. Guilmain, S. Machinani, J. Kotula, S. Saha, P. Miller, A. M. Brennan, Translational development of microbiome-based therapeutics: Kinetics of *E. coli* Nissle and engineered strains in humans and nonhuman primates. *Clin. Transl. Sci.* **11**, 200–207 (2018).
41. W. Kruis, E. Schütz, P. Fric, B. Fixa, G. Judmaier, M. Stolte, Double-blind comparison of an oral *Escherichia coli* preparation and mesalazine in maintaining remission of ulcerative colitis. *Aliment. Pharmacol. Ther.* **11**, 853–858 (1997).
42. W. Kruis, P. Frič, J. Pokrotnieks, M. Lukás, B. Fixa, M. Kaščák, M. A. Kamm, J. Weismueller, C. Beglinger, M. Stolte, C. Wolff, J. Schulze, Maintaining remission of ulcerative colitis with the probiotic *Escherichia coli* Nissle 1917 is as effective as with standard mesalazine. *Gut* **53**, 1617–1623 (2004).
43. B. J. Rembacken, A. M. Snelling, P. M. Hawkey, D. M. Chalmers, A. T. R. Axon, Non-pathogenic *Escherichia coli* versus mesalazine for the treatment of ulcerative colitis: A randomised trial. *Lancet* **354**, 635–639 (1999).
44. W. Kruis, S. Chrubasik, S. Boehm, C. Stange, J. Schulze, A double-blind placebo-controlled trial to study therapeutic effects of probiotic *Escherichia coli* Nissle 1917 in subgroups of patients with irritable bowel syndrome. *Int. J. Colorectal Dis.* **27**, 467–474 (2012).
45. J. Häberle, N. Boddaert, A. Burlina, A. Chakrapani, M. Dixon, M. Huemer, D. Karall, D. Martinelli, P. S. Crespo, R. Santer, A. Servais, V. Valayannopoulos, M. Lindner, V. Rubio, C. Dionisi-Vici, Suggested guidelines for the diagnosis and management of urea cycle disorders. *Orphanet J. Rare Dis.* **7**, 32 (2012).
46. C. J. McNeal, C. J. Meininger, D. Reddy, C. D. Wilborn, G. Wu, Safety and effectiveness of arginine in adults. *J. Nutr.* **146**, 2587S–2593S (2016).
47. E. Sancho-Vaello, M. L. Fernandez-Murga, V. Rubio, Mechanism of arginine regulation of acetylglutamate synthase, the first enzyme of arginine synthesis. *FEBS Lett.* **583**, 202–206 (2009).
48. G. Zhao, Z. Jin, N. M. Allewell, M. Tuchman, D. Shi, Crystal structure of the *N*-acetyltransferase domain of human *N*-acetyl-L-glutamate synthase in complex with *N*-acetyl-L-glutamate provides insights into its catalytic and regulatory mechanisms. *PLOS ONE* **8**, e70369 (2013).
49. S. Durand, G. Storz, Reprogramming of anaerobic metabolism by the FnrS small RNA. *Mol. Microbiol.* **75**, 1215–1231 (2010).
50. A. Boysen, J. Møller-Jensen, B. Kallipolitis, P. Valentin-Hansen, M. Overgaard, Translational regulation of gene expression by an anaerobically induced small non-coding RNA in *Escherichia coli*. *J. Biol. Chem.* **285**, 10690–10702 (2010).
51. S. I. Ahmad, S. H. Kirk, A. Eisenstark, Thymine metabolism and thymineless death in prokaryotes and eukaryotes. *Annu. Rev. Microbiol.* **52**, 591–625 (1998).
52. U.S. Department of Health and Human Services, Food and Drug Administration Guidance for Industry, "Early clinical trials with live biotherapeutic products: Chemistry, manufacturing, and control information," February 2012; www.fda.gov/downloads/Biologi%E2%80%A6/UCM292704.pdf [updated June 2016].
53. M. I. Love, W. Huber, S. Anders, Moderated estimation of fold change and dispersion for RNA-seq data with DESeq2. *Genome Biol.* **15**, 550 (2014).
54. M. Fulde, J. Willenborg, A. de Greeff, L. Benga, H. E. Smith, P. Valentin-Weigand, R. Goethe, ArgR is an essential local transcriptional regulator of the *arcABC* operon in *Streptococcus suis* and is crucial for biological fitness in an acidic environment. *Microbiology* **157**, 572–582 (2011).
55. C.-D. Lu, H. Winteler, A. Abdelal, D. Haas, The ArgR regulatory protein, a helper to the anaerobic regulator ANR during transcriptional activation of the *arcD* promoter in *Pseudomonas aeruginosa*. *J. Bacteriol.* **181**, 2459–2464 (1999).
56. A. Battesti, N. Majdalani, S. Gottesman, The RpoS-mediated general stress response in *Escherichia coli*. *Annu. Rev. Microbiol.* **65**, 189–213 (2011).
57. F. Arsène, T. Tomoyasu, B. Bukau, The heat shock response of *Escerichia coli*. *Int. J. Food Microbiol.* **55**, 3–9 (2000).
58. M.-P. Castanié-Cornet, K. Cam, B. Bastiat, A. Cros, P. Bordes, C. Gutierrez, Acid stress response in *Escherichia coli*: Mechanism of regulation of *gadA* transcription by RcsB and GadE. *Nucleic Acids Res.* **38**, 3546–3554 (2010).
59. Y. C. Luiking, N. E. P. Deutz, Biomarkers of arginine and lysine excess. *J. Nutr.* **137**, 1662S–1668S (2007).
60. P. E. Hodges, L. E. Rosenberg, The spf$^{ash}$ mouse: A missense mutation in the ornithine transcarbamylase gene also causes aberrant mRNA splicing. *Proc. Natl. Acad. Sci. U.S.A.* **86**, 4142–4146 (1989).
61. D. T. Riglar, P. A. Silver, Engineering bacteria for diagnostic and therapeutic applications. *Nat. Rev. Microbiol.* **16**, 214–225 (2018).
62. H. Braat, P. Rottiers, D. W. Hommes, N. Huyghebaert, E. Remaut, J.-P. Remon, S. J. H. van Deventer, S. Neirynck, M. P. Peppelenbosch, L. Steidler, A phase I trial with transgenic bacteria expressing interleukin-10 in Crohn's disease. *Clin. Gastroenterol. Hepatol.* **4**, 754–759 (2006).
63. S. A. Limaye, R. I. Haddad, F. Cilli, S. T. Sonis, A. D. Colevas, M. T. Brennan, K. S. Hu, B. A. Murphy, Phase 1b, multicenter, single blinded, placebo-controlled, sequential dose escalation study to assess the safety and tolerability of topically applied AG013 in subjects with locally advanced head and neck cancer receiving induction chemotherapy. *Cancer* **119**, 4268–4276 (2013).
64. E. G. Pamer, Immune responses to *Listeria monocytogenes*. *Nat. Rev. Immunol.* **4**, 812–823 (2004).
65. R. Okazaki, A. Kornberg, Deoxythymidine kinase of *Escherichia coli*. I. Purification and some properties of the enzyme. *J. Biol. Chem.* **239**, 269–274 (1964).
66. B. A. McCullough, M. Yudkoff, M. L. Batshaw, J. M. Wilson, S. E. Raper, M. Tuchman, Genotype spectrum of ornithine transcarbamylase deficiency: Correlation with the clinical and biochemical phenotype. *Am. J. Med. Genet.* **93**, 313–319 (2000).
67. A. L. Gropman, M. Summar, J. V. Leonard, Neurological implications of urea cycle disorders. *J. Inherit. Metab. Dis.* **30**, 865–879 (2007).
68. B. Parmeggiani, C. R. Vargas, Oxidative stress in urea cycle disorders: Findings from clinical and basic research. *Clin. Chim. Acta* **477**, 121–126 (2018).
69. R. F. Butterworth, M. D. Norenberg, V. Felipo, P. Ferenci, J. Albrecht, A. T. Blei, Experimental models of hepatic encephalopathy: ISHEN guidelines. *Liver Int.* **29**, 783–788 (2009).
70. R. K. Dhiman, B. Rana, S. Agrawal, A. Garg, M. Chopra, K. K. Thumburu, A. Khattri, S. Malhotra, A. Duseja, Y. K. Chawla, Probiotic VSL#3 reduces liver disease severity and hospitalization in patients with cirrhosis: A randomized, controlled trial. *Gastroenterology* **147**, 1327–1337.e3 (2014).
71. S. Wang, M. Xu, W. Wang, X. Cao, M. Piao, S. Khan, F. Yan, H. Cao, B. Wang, Systematic review: Adverse events of fecal microbiota transplantation. *PLOS ONE* **11**, e0161174 (2016).
72. U. Sonnenborn, J. Schulze, The non-pathogenic *Escherichia coli* strain Nissle 1917—Features of a versatile probiotic. *Microb. Ecol. Health Dis.* **21**, 122–158 (2009).
73. E. van Nood, A. Vrieze, M. Nieuwdorp, S. Fuentes, E. G. Zoetendal, W. M. de Vos, C. E. Visser, E. J. Kuijper, J. F. W. M. Bartelsman, J. G. P. Tijssen, P. Speelman, M. G. W. Dijkgraaf, J. J. Keller, Duodenal infusion of donor feces for recurrent *Clostridium difficile*. *N. Engl. J. Med.* **368**, 407–415 (2013).
74. Q. Liu, Z. P. Duan, D. K. Ha, S. Bengmark, J. Kurtovic, S. M. Riordan, Synbiotic modulation of gut flora: Effect on minimal hepatic encephalopathy in patients with cirrhosis. *Hepatology* **39**, 1441–1449 (2004).
75. A. A. Zyrek, C. Cichon, S. Helms, C. Enders, U. Sonnenborn, M. A. Schmidt, Molecular mechanisms underlying the probiotic effects of *Escherichia coli* Nissle 1917 involve ZO-2 and PKCζ redistribution resulting in tight junction and epithelial barrier repair. *Cell. Microbiol.* **9**, 804–816 (2007).
76. Y. Dagon, Y. Millet, L. Renaud, B. Ha, D. Wong, M. Castillo, J. Thomas, J. Lora, P. Miller, C. Kurtz, Genetically engineered *E. coli* Nissle attenuates hyperammonemia in a mouse model of hepatic encephalopathy by metabolizing gut ammonia and increasing urea production. *Gastroenterology* **154**, S-1078 (2018).
77. S. M. Morris Jr., Arginine metabolism revisited. *J. Nutr.* **146**, 2579S–2586S (2016).
78. F. Mariotti, K. J. Petzke, D. Bonnet, I. Szezepanski, C. Bos, J.-F. Huneau, H. Fouillet, Kinetics of the utilization of dietary arginine for nitric oxide and urea synthesis: Insight into the arginine-nitric oxide metabolic system in humans. *Am. J. Clin. Nutr.* **97**, 972–979 (2013).
79. C. D. Leaf, J. S. Wishnok, S. R. Tannenbaum, L-arginine is a precursor for nitrate biosynthesis in humans. *Biochem. Biophys. Res. Commun.* **163**, 1032–1037 (1989).
80. L. Castillo, T. C. deRojas, T. E. Chapman, J. Vogt, J. F. Burke, S. R. Tannenbaum, V. R. Young, Splanchnic metabolism of dietary arginine in relation to nitric oxide synthesis in normal adult man. *Proc. Natl. Acad. Sci. U.S.A.* **90**, 193–197 (1993).
81. J. A. Sawitzke, L. C. Thomason, N. Costantino, M. Bubunenko, S. Datta, D. L. Court, Recombineering: In vivo genetic engineering in *E. coli*, *S. enterica*, and beyond. *Methods Enzymol.* **421**, 171–199 (2007).

82. M. K. Thomason, T. Bischler, S. K. Eisenbart, K. U. Förstner, A. Zhang, A. Herbig, K. Nieselt, C. M. Sharma, G. Storz, Global transcriptional start site mapping using differential RNA sequencing reveals novel antisense RNAs in *Escherichia coli*. *J. Bacteriol.* **197**, 18–28 (2015).
83. M. R. Charbonneau, D. O'Donnell, L. V. Blanton, S. M. Totten, J. C. C. Davis, M. J. Barratt, J. Cheng, J. Guruge, M. Talcott, J. R. Bain, M. J. Muehlbauer, O. Ilkayeva, C. Wu, T. Struckmeyer, D. Barile, C. Mangani, J. Jorgensen, Y.-m. Fan, K. Maleta, K. G. Dewey, P. Ashorn, C. B. Newgard, C. Lebrilla, D. A. Mills, J. I. Gordon, Sialylated milk oligosaccharides promote microbiota-dependent growth in models of infant undernutrition. *Cell* **164**, 859–871 (2016).
84. A. M. Bolger, M. Lohse, B. Usadel, Trimmomatic: A flexible trimmer for Illumina sequence data. *Bioinformatics* **30**, 2114–2120 (2014).
85. M. Reister, K. Hoffmeier, N. Krezdorn, B. Rotter, C. Liang, S. Rund, T. Dandekar, U. Sonnenborn, T. A. Oelschlaeger, Complete genome sequence of the Gram-negative probiotic *Escherichia coli* strain Nissle 1917. *J. Biotechnol.* **187**, 106–107 (2014).
86. B. Langmead, C. Trapnell, M. Pop, S. L. Salzberg, Ultrafast and memory-efficient alignment of short DNA sequences to the human genome. *Genome Biol.* **10**, R25 (2009).
87. S. Anders, P. T. Pyl, W. Huber, HTSeq—A Python framework to work with high-throughput sequencing data. *Bioinformatics* **31**, 166–169 (2015).
88. M. Kanehisa, Y. Sato, M. Kawashima, M. Furumichi, M. Tanabe, KEGG as a reference resource for gene and protein annotation. *Nucleic Acids Res.* **44**, D457–D462 (2016).
89. M. C. Wallace, K. Hamesch, M. Lunova, Y. Kim, R. Weiskirchen, P. Strnad, S. L. Friedman, Standard operating procedures in experimental liver research: Thioacetamide model in mice and rats. *Lab. Anim* **49**, 21–29 (2015).
90. M. Yudkoff, Y. Daikhin, I. Nissim, A. Jawad, J. Wilson, M. Batshaw, In vivo nitrogen metabolism in ornithine transcarbamylase deficiency. *J. Clin. Invest.* **98**, 2167–2173 (1996).


**Acknowledgments:** We would like to thank M. Castillo, C. Fox, B. Ha, D. Wong, L. Renaud, K. Li, N. Li, C. Bergeron, M. Momin, L. Lorenzo, and T. Kane for technical and editorial support. **Funding:** Funding for the enclosed studies was provided by Synlogic Inc. **Author contributions:** C.B.K., Y.A.M., M.K.P., M.P., M.R.C., and V.M.I. contributed to the design of experiments, analysis of data, and writing of manuscript. J.W.K., Y.D., and K.A.W. developed strains and conducted experiments. A.J.D. conducted qPCR and analyzed results. W.S.D. and D.A.W. designed studies and conducted data analysis on clinical results. E.A. developed the fermentation process and formulation for the phase 1 study with SYNB1020. P.F.M. and A.M.B. contributed to design and interpretation of study results. **Competing interests:** C.B.K., Y.A.M., M.K.P., M.P., M.R.C., V.M.I., J.W.K., Y.D., K.A.W., P.F.M., and A.M.B were all employees and shareholders of Synlogic Inc. at the time these studies were conducted. Synlogic owns issued and pending patents encompassing SYNB1020. W.S.D. was a consultant to Synlogic Inc. at the time these studies were conducted. **Data and materials availability:** Engineered strains described in this manuscript can be made available through a materials transfer agreement with Synlogic Inc. Correspondence should be addressed to Vincent Isabella (vincent@synlogictx.com). RNA sequencing data are available in the European Nucleotide Archive, under accession PRJEB27637. All data associated with this study are present in the paper or in the Supplementary Materials.

Submitted 16 July 2018
Resubmitted 8 October 2018
Accepted 19 December 2018
Published 16 January 2019
10.1126/scitranslmed.aau7975

**Citation:** C. B. Kurtz, Y. A. Millet, M. K. Puurunen, M. Perreault, M. R. Charbonneau, V. M. Isabella, J. W. Kotula, E. Antipov, Y. Dagon, W. S. Denney, D. A. Wagner, K. A. West, A. J. Degar, A. M. Brennan, P. F. Miller, An engineered *E. coli* Nissle improves hyperammonemia and survival in mice and shows dose-dependent exposure in healthy humans. *Sci. Transl. Med.* **11**, eaau7975 (2019).

Science Translational Medicine

# An engineered *E. coli* Nissle improves hyperammonemia and survival in mice and shows dose-dependent exposure in healthy humans

Caroline B. Kurtz, Yves A. Millet, Marja K. Puurunen, Mylène Perreault, Mark R. Charbonneau, Vincent M. Isabella, Jonathan W. Kotula, Eugene Antipov, Yossi Dagon, William S. Denney, David A. Wagner, Kip A. West, Andrew J. Degar, Aoife M. Brennan and Paul F. Miller

*Sci Transl Med* **11**, eaau7975.
DOI: 10.1126/scitranslmed.aau7975

**An anti-ammonia probiotic**

Hyperammonemia, or excess blood ammonia, is a serious condition that can result in brain damage and death. In pursuit of a potential therapeutic, Kurtz *et al.* modified the metabolism of a probiotic *E. coli* strain to overproduce arginine, thereby sequestering some of the ammonia produced by gut bacteria into the amino acid molecules. The engineered strain, called SYNB1020, lowered blood ammonia, increased survival in mouse hyperammonemia models, and showed repeat-dose tolerability in nonhuman primates. A phase 1 dose-escalation study in healthy human volunteers resulted in no serious adverse events and indicated that the bacterium was metabolically active in vivo, suggesting that SYNB1020 warrants further clinical development.